Filomat 38:8 (2024), 2949–2963
https://doi.org/10.2298/FIL2408949V

Published by Faculty of Sciences and Mathematics,
University of Niš, Serbia
Available at: http://www.pmf.ni.ac.rs/filomat

A fast Taylor-wavelet based numerical algorithm for the solution of HIV-infected $CD4^+T$ cells model

Vivek[a], Manoj Kumar[a,*], Suyash Narayan Mishra[a]

[a] *Applied Sciences and Humanities Department, Institute of Engineering and Technology, Dr. A.P.J. Abdul Kalam Technical University, Lucknow-226021, Uttar Pradesh, India*

Abstract. In this article, we present a novel approach under the Taylor wavelet and collocation technique which is computationally efficient to obtain the solution of the model of $CD4^+T$ cells of HIV infection. A system of nonlinear ordinary differential equations represents this mathematical model. On applying the proposed technique described in this article, we have transformed this model into algebraic form and then simplified using a suitable method. The suggested Taylor wavelet approach is worked out for the convergence analysis and thereafter it is also demonstrated that the Taylor wavelet expansion of a function converges uniformly to itself. It is anticipated that the proposed approach would be more efficient and suitable for solving a variety of nonlinear ordinary and partial differential equations that occur in various such models of medical science and engineering. Tables and graphs are included to show how the suggested wavelet method provides enhanced accuracy for a wide range of problems. Relative data and computations are performed over MATLAB software.

1. Introduction

Mathematics provides a powerful tool for understanding and solving a wide range of real-world problems. For instance, we developed a model to explain biological elements like a human immunodeficiency virus infection (HIV). Viruses have evolved various strategies to enter live cells, infect the host cell, and evade the host immune system. Understanding these mechanisms is crucial in combating viral infections. the activation of pattern-recognition receptors (PRRs) plays a pivotal role in triggering innate immune responses against pathogens, including viruses. When pathogens, such as viruses, connect to PRRs, it sets off a cascade of events that initiate the body's natural immune defense mechanisms. Adaptive immunological responses play a crucial role in triggering the immune system's development of effector cells. The adaptive immune system is a specialized branch of the immune system responsible for mounting highly targeted and specific responses to pathogens, including viruses. Alan Perelson, a renowned mathematical biologist and immunologist, developed a mathematical model [1] of HIV infection in 1989. Perelson's model is a fundamental representation of how the human immunodeficiency virus (HIV) propagates in the human body and how it interacts with the immune system. Leukocytes, commonly known as white blood cells, are

2020 *Mathematics Subject Classification*. Primary 34A34, 65L05
Keywords. $CD4^+T$ HIV infection model, Taylor wavelet, Collocation technique, Nonlinear ODEs, MATLAB
Received: 15 April 2023; Revised: 09 October 2023; Accepted: 25 October 2023
Communicated by Miodrag Spalević
* Corresponding author: Manoj Kumar
Email addresses: 2100522007101@ietlucknow.ac.in (Vivek), manojkumar@ietlucknow.ac.in (Manoj Kumar), snmishra@ietlucknow.ac.in (Suyash Narayan Mishra)

indeed fundamental components of the human immune system (HIS). However, it's important to clarify that while leukocytes include various types of white blood cells, CD4+ T cells are a specific subset of white blood cells with crucial roles in the immune system.

1.1. Global HIV report and statistics

Understanding and studying the HIV infection model is crucial because acquired immunodeficiency syndrome (AIDS), which is the advanced stage of HIV infection, has significant and far-reaching impacts on individual health and public health. The UNAIDS 2018 report highlights the global impact of HIV/AIDS. The estimated number of people worldwide who were living with HIV at that time was 37.9 Million people Living with HIV, the number of individuals who were receiving antiretroviral therapy (ART) was 23.3 Million, and the estimated number of new HIV infections that occurred during that year was 1.7 Million [2].

1. In 2021, there were an estimated 36.7 million adults living with HIV and 1.7 million children (aged 15 and under) living with HIV.
2. Among the total number of individuals living with HIV in 2021, approximately 54% were women and girls.

It's important to note that these statistics emphasize the ongoing need for global collaboration and resources dedicated to addressing HIV/AIDS and its associated health challenges. Many of the nations most affected by HIV are also grappling with a range of other critical health and socioeconomic issues. This intersection of HIV/AIDS with other challenges can exacerbate the overall impact on affected populations specifically coexisting infectious diseases, healthcare infrastructure, food insecurity, economic challenges, population mobility, etc. Literally, over the past few decades, a significant amount of research has been dedicated to understanding HIV/AIDS, developing effective treatments, and devising strategies for HIV prevention. The modeling of HIV dynamics and the assessment of various therapies are of significant interest to researchers in the field of biomathematics. Mathematical modeling plays a crucial role in understanding the complex dynamics of HIV infection, evaluating the efficacy of different treatment strategies, and predicting the long-term outcomes of interventions. Numerical approaches are essential for examining and analyzing mathematical models of complex biological systems, including models of HIV dynamics and its therapies. These numerical methods allow researchers to approximate solutions to differential equations and simulate the behavior of the system over time.
Consider the biological model of HIV infection of the $CD4^+T$ cells of the form:

$$\left\{\begin{array}{c} \frac{\mathrm{dX}}{\mathrm{d}\beta} = \rho - \alpha X + \kappa X\left(1 - \frac{X+Y}{X_{Max}}\right) - \eta XZ \\ \frac{dY}{d\beta} = \eta XZ - eY \\ \frac{dZ}{d\beta} = Yle - \zeta Z \end{array}\right\}, \tag{1}$$

under the intial conditions $X(0) = 0.1$, $Y(0) = 0$, and $Z(0) = 0.1$.
The parameters involved are used for;

$X(\beta)$ = The concentration of uninfected $CD4^+$T cells (per unit volume) at time β,
$Y(\beta)$ =The concentration of infected $CD4^+$T cells (per unit volume) at time β,
$Z(\beta)$ =The concentration of free virus particles (per unit volume) at time β,
α = Natural turnover rates of uninfected $CD4^+T$ cells
e = Infected $CD4^+$T cells
ζ = Virus particles
ηXZ = HIV infection of healthy $CD4^+$T cells
X_{max} = Maximum $CD4^+$T cells in the body
$\left(1 - \frac{X+Y}{X_{max}}\right)$ = Logistic development of the healthy $CD4^+$T cells.

Let's say that the infection rate is represented by the real number η in the infectious body of a person, and the values of the parameters that happened in this system as follows: $\rho = 0.1$, $\alpha = 0.02, e = 0.3, \kappa = 3, \zeta = 2.4, \eta = 0.0027, X_{\max} = 1500, l = 9$. Numerous numerical methods have been introduced to tackle the model of HIV infected $CD4^{+}T$ cells and other problems of significant interest. For instance, the operational matrix of Bessel polynomials [3], HPM technique [5], Homotopy method for HIV infection model [4], LADM approach for HIV infection model [6], LSCA for HIV infection model [7], MDTM for fractional HIV infection model [8], MVIM for HIV infection model [9], SLCM for HIV infection model [10], BCM for HIV infection model [11, 12], and on the modeling and analysis of HIV infection and other applied problems by means of the wavelet and collocation techniques are addressed such as [23] developed a novel model for infection, [24] proposed a novel method for nonlinear PDEs, [25] proposed a novel clique collection method for the fractional model, [26] proposed a B-spline and Jacobi method for nonlinear PDEs, [27] solved a Heat transfer model using Fibonacci wavelets represented by nonlinear PDEs, [28] solved a fractional order model using Legendre spectral method, [29] solved a fractional order Integro-differential equations model using the collocation method, [30] studied the HIV Latent Reservoir in HIV Infection and others [35–37].

1.2. Wavelets in Numerical Analysis

Wavelet algorithms have indeed gained attention from researchers in the field of numerical analysis and computational mathematics for solving a wide range of linear and nonlinear ordinary and partial differential equations (ODEs and PDEs). Wavelets are capable of representing functions at multiple levels of resolution or detail. This multiresolution property allows for adaptive refinements in regions where fine-scale information is needed while maintaining a coarser representation elsewhere. It is particularly useful in capturing localized features in differential equations. Due to these features, wavelet-based numerical approaches have gained popularity for solving Integral equations [20], including both ordinary and partial differential equations. Wavelet-based numerical methods are extensively applied in [24] and [22]. Little research is known that uses wavelets to address the HIV mathematical model so this impetus us to use the Taylor wavelet collocation method (TWCM).

Wavelet bases have indeed found applications in various real-life mathematical models across different fields. These applications leverage the adaptivity, accuracy, and efficiency of wavelets to address complex problems as in BWM Bernoulli wavelet method [13]-[16], operational matrix of integration for the IDEs [14], Numerical solution using Haar wavelet [15–17], MTF equations using Hermite [18], solution of singular differential equations [33], and Fibonacci wavelet method [32]etc.

The primary objective of this paper is to present and explore the Taylor wavelet collocation technique (TWCM), which uses the Taylor wavelet basis to learn more about the numerical and geometrical behavior of a nonlinear mathematical representation. Only a few of the approaches that have been explored previously explained for dealing with this mathematical structure include the R-K technique, Haar wavelet technique, Laplace Adomian Decomposition method (LADM), LADM Pade, The Homotopy analysis approach, Differential transform method, multistep Adomian decomposition method, modified variational iteration method, Runge-Kutta, and other semi-analytic techniques. Although these techniques were accurate and effective, TWCM offers an approach that is more exact. The research presented in this publication is absolutely new and has never been done before. With this strategy, difficult numerical techniques are removed, and useful data about the model's numerical behavior is generated. The problem is also resolved via numerical computing using the provided approach. By comparing our strategy to the existing work, the accuracy and proficiency of the recommended technique are shown.

Following is an overview of this article: We explain the characteristics of the Taylor wavelets and the approximation of a function using the Taylor wavelet basis in Section 2. Section 3 presents a fundamental concept for approximating a function while Section 4 provides a convergence analysis of the method. In Section 5, we discuss how to use the Taylor wavelets to generate the operational matrix of integration. In Section 6, we provide the methodology for the proposed method using Taylor wavelets. Application of the method to the given problem and comparison with the previous work has been discussed in Section 7. In Section 8, an overall conclusion is drawn.

2. Taylor wavelets

A family of functions generated by the translation and dilation of a single function which is known as the "mother wavelet" is called the wavelets. Let x and y be two continuous parameters that stand for dilation and translation then we define the continuous family of wavelets as;

$$\Phi_{x,y}(\beta) = |x|^{-1/2}\Phi\left(\frac{\beta - y}{x}\right), \forall x, y \in \mathbb{R}, x \neq 0. \tag{2}$$

If we choose $x = x_0^{-\theta}, y = \omega x_0^{-\theta} y_0, x_0 > 1, y_0 > 1$, and ω and θ are positive integers, the discrete wavelet family is introduced as,

$$\Phi_{\theta,\omega}(\beta) = |x_0|^{\frac{\theta}{2}}\,\Phi\left(x_0^{\theta}\beta - \omega y_0\right),$$

where $\Phi_{\theta,\omega}(\beta)$ is the wavelet basis in $L^2(\mathbb{R})$. Further wavelets family $\Phi_{\theta,\omega}(\beta)$ represents an orthonormal basis for the fixed values of $x_0 = 2$ and $y_0 = 1$.

2.1. Taylor wavelets

Taylor wavelets [32, 34] are defined under four arguments as $\Phi_{\omega,r}(\beta) = \Phi(\theta, \hat{\omega}, r, \beta)$: $\hat{\omega} = \omega - 1$, $\omega = 1, 2, \ldots, 2^{\theta-1}$. Consider the following collection of functions defined on $[0, 1]$:

$$\Phi_{\omega,r}(\beta) = \begin{cases} 2^{\frac{\theta-1}{2}}\tilde{L}_r\left(2^{\theta-1}\beta - \hat{\omega}\right), & \frac{\hat{\omega}}{2^{\theta-1}} \leq \beta < \frac{\hat{\omega}+1}{2^{\theta-1}} \\ 0, & \text{otherwise} \end{cases} \tag{3}$$

with

$$\tilde{L}_r(\beta) = \sqrt{2r+1}L_r(\beta),$$

where $\Phi_{\omega,r}(\beta)$ are defined as the Taylor wavelets and $L_r(\beta) = \beta^r$ is the well-known Taylor polynomials of order r for $r = 0, 1, 2, \ldots, \mathbb{M} - 1$. The coefficient $\sqrt{2r+1}$ is for normality, the dilation parameter is $x = 2^{-(\theta-1)}$ and the translation parameter is $y = \hat{\omega}2^{-(\theta-1)}$.

3. Approximation of function

Consider a function $\Lambda \in L^2[0, 1]$ then we can represent it as;

$$\Lambda(\beta) = \sum_{\omega=1}^{\infty}\sum_{r=0}^{\infty} a_{\omega,r}\Phi_{\omega,r}(\beta), \tag{4}$$

where $\Phi_{\omega,r}$ stands for the Taylor wavelets basis and $a_{\omega,r} = \langle \Lambda(\beta), \Phi_{\omega,r} \rangle$ are the unknown coefficients. Assume the truncated series of the $\Lambda(\beta)$:

$$\Lambda(\beta) \simeq \sum_{\omega=1}^{2^{\theta-1}}\sum_{r=0}^{\mathbb{M}-1} a_{\omega,r}\Phi_{\omega,r}(\beta) = E^T\Phi(\beta) = \Lambda_n(\beta), \tag{5}$$

where E, $\Phi(\beta)$ are $n \times 1$ $\left(n = 2^{\theta-1}\mathbb{M}\right)$ matrices defined as;

$$\begin{aligned} E &= \left[a_{1,0}, a_{1,1}, \ldots, a_{1,\mathbb{M}-1}, a_{2,0}, \ldots, a_{2,\mathbb{M}-1}, \ldots, a_{2^{\theta-1},0}, \ldots, a_{2^{\theta-1},\mathbb{M}-1}\right]^T, \\ \Phi(\beta) &= \left[\Phi_{1,0}(\beta), \Phi_{1,1}(\beta), \ldots, \Phi_{1,\mathbb{M}-1}(\beta), \Phi_{2,0}(\beta), \ldots, \Phi_{2,\mathbb{M}-1}(\beta), \ldots, \Phi_{2^{\theta-1},0}(\beta), \ldots, \Phi_{2^{\theta-1},\mathbb{M}-1}(\beta)\right]^T. \end{aligned} \tag{6}$$

4. Convergence analysis

This section presents two main theorems related to the analysis of convergence and absolute error;

Theorem 1. Let $\Lambda(\beta) \in L^2(\mathbb{R})$ be a continuous function on the interval $[0,1)$ such that it is bounded by δ i.e. $|\Lambda(\beta)| < \delta$, for every $\beta \in [0,1)$. Then, the Taylor wavelet coefficients of $\Lambda(\beta)$ in Eq. (5) are bounded as:

$$\left|a_{\omega,r}\right| < \frac{\lambda}{2^{\frac{\theta-1}{2}}}\delta\frac{2}{2r+1},$$

where δ is a constant and λ is given by

$$\lambda = \sqrt{2r+1}.$$

Proof. See [33]

Theorem 2. Let $\Lambda(\beta) \in L^2(\mathbb{R})$ be a continuous function on the interval $[0,1)$ and $|\Lambda(\beta)| < \delta$ for every $\beta \in [0,1)$. Let $\Lambda^*(\beta) = \sum_{\omega=1}^{2^{\theta-1}} \sum_{r=0}^{\mathbb{M}-1} a_{\omega,r}\Phi_{\omega,r}(\beta)$ be the Taylor wavelet series expansions where $a_{\omega,r}$, $\Phi_{\omega,r}(\beta)$ be the Taylor wavelet coefficients and Taylor wavelet basis respectively. Then, the bound of the truncated error $e(\beta)$ is given as:

$$\|e(\beta)\|_2 = \left\|\Lambda(\beta) - \Lambda^*(\beta)\right\| < \left(\sum_{\omega=2^{\theta-1}+1}^{\infty}\sum_{r=0}^{\mathbb{M}-1} a_{\omega,r}^2\right)^{\frac{1}{2}} + \left(\sum_{\omega=1}^{\infty}\sum_{r=\mathbb{M}}^{\infty} a_{\omega,r}^2\right)^{\frac{1}{2}},$$

where,

$$a_{\omega,r} = \frac{\lambda}{2^{\frac{\theta-1}{2}}}\delta\frac{2}{2r+1},\ \lambda = \sqrt{2r+1}.$$

Proof. See [33]

5. Operational matrix of integration

Let us consider some initial Taylor wavelet basis to generate an integration operator matrix for $\theta = 1$ and $2^{\theta-1}\mathbb{M} = n = 6$:

$$\begin{aligned}
&\Phi_{1,0}(\beta) = 1,\\
&\Phi_{1,1}(\beta) = \sqrt{3}\beta,\\
&\Phi_{1,2}(\beta) = \sqrt{5}\beta^2,\\
&\Phi_{1,3}(\beta) = \sqrt{7}\beta^3,\\
&\Phi_{1,4}(\beta) = \sqrt{9}\beta^4,\\
&\Phi_{1,5}(\beta) = \sqrt{11}\beta^5.\\
&\text{Let } \Phi(\beta) = \left[\Phi_{1,0}(\beta),\ \Phi_{1,1}(\beta),\ \Phi_{1,2}(\beta),\ \Phi_{1,3}(\beta),\ \Phi_{1,4}(\beta),\ \Phi_{1,5}(\beta)\right].
\end{aligned}$$

Now integrate each basis element with respect to β from 0 to β and then express them as a linear combination to obtain the following vector form expression;

$$\int_0^\beta \Phi_{1,0}(\beta)d\beta = \begin{bmatrix} 0 & \frac{1}{\sqrt{3}} & 0 & 0 & 0 & 0 \end{bmatrix}\Phi_6(\beta),$$
$$\int_0^\beta \Phi_{1,1}(\beta)d\beta = \begin{bmatrix} 0 & 0 & \frac{\sqrt{3}}{2\sqrt{5}} & 0 & 0 & 0 \end{bmatrix}\Phi_6(\beta),$$
$$\int_0^\beta \Phi_{1,2}(\beta)d\beta = \begin{bmatrix} 0 & 0 & 0 & \frac{\sqrt{5}}{3\sqrt{7}} & 0 & 0 \end{bmatrix}\Phi_6(\beta),$$
$$\int_0^\beta \Phi_{1,3}(\beta)d\beta = \begin{bmatrix} 0 & 0 & 0 & 0 & \frac{\sqrt{7}}{4\sqrt{9}} & 0 \end{bmatrix}\Phi_6(\beta),$$
$$\int_0^\beta \Phi_{1,4}(\beta)d\beta = \begin{bmatrix} 0 & 0 & 0 & 0 & 0 & \frac{\sqrt{9}}{5\sqrt{11}} \end{bmatrix}\Phi_6(\beta),$$
$$\int_0^\beta \Phi_{1,5}(\beta)d\beta = \begin{bmatrix} 0 & 0 & 0 & 0 & 0 & 0 \end{bmatrix}\Phi_6(\beta) + \frac{\sqrt{11}}{6\sqrt{13}}\overline{\Phi_{1,6}}(\beta).$$

Therefore, we obtain

$$\int_0^\beta \Phi(\beta)d\beta = P_{6\times6}\Phi_6(\beta) + \overline{\Phi_6}(\beta), \tag{7}$$

here $P_{6\times6}$ is the required operational matrix of integration and given as;

$$P_{6\times6} = \begin{bmatrix} 0 & \frac{1}{\sqrt{3}} & 0 & 0 & 0 & 0 \\ 0 & 0 & \frac{\sqrt{3}}{2\sqrt{5}} & 0 & 0 & 0 \\ 0 & 0 & 0 & \frac{\sqrt{5}}{3\sqrt{7}} & 0 & 0 \\ 0 & 0 & 0 & 0 & \frac{\sqrt{7}}{4\sqrt{9}} & 0 \\ 0 & 0 & 0 & 0 & 0 & \frac{\sqrt{9}}{5\sqrt{11}} \\ 0 & 0 & 0 & 0 & 0 & 0 \end{bmatrix}$$

with

$$\overline{\Phi_6}(\beta) = \begin{bmatrix} 0 \\ 0 \\ 0 \\ 0 \\ 0 \\ \frac{\sqrt{11}}{6\sqrt{13}}\overline{\Phi_{1,6}}(\beta) \end{bmatrix}.$$

The same process can be adapted to proceed to generate an operational matrix of integration for any order $n \times n$.

6. Methodology

This section presents the strategy of application of the proposed method for the HIV infection model of $CD4^+$T cells.

Consider,

$$\frac{dX}{d\beta} = R^T\Phi(\beta) \tag{8}$$

$$\frac{dY}{d\beta} = S^T\Phi(\beta) \tag{9}$$

$$\frac{dZ}{d\beta} = T^T\Phi(\beta) \tag{10}$$

where,

$$R^T = \left[rx_{1,0}, \ldots rx_{1,\mathbb{M}-1}, rx_{2,0}, \ldots rx_{2,\mathbb{M}-1}, rx_{2^{\theta-1},0}, \ldots rx_{2^{\theta-1},\mathbb{M}-1}\right],$$
$$S^T = \left[sy_{1,0}, \ldots sy_{1,\mathbb{M}-1}, sy_{2,0}, \ldots sy_{2,\mathbb{M}-1}, sy_{2^{\theta-1},0}, \ldots sy_{2^{\theta-1},\mathbb{M}-1}\right],$$
$$T^T = \left[tz_{1,0}, \ldots tz_{1,\mathbb{M}-1}, tz_{2,0}, \ldots tz_{2,\mathbb{M}-1}, tz_{2^{\theta-1},0}, \ldots tz_{2^{\theta-1},\mathbb{M}-1}\right],$$

are the unknown coefficients vector and $\Phi(\beta) = \left[\Phi_{1,0}(\beta), \ldots \Phi_{1,\mathbb{M}-1}(\beta), \Phi_{2,0}(\beta), \ldots \Phi_{2,\mathbb{M}-1}(\beta), \Phi_{2^{\theta-1},0}(\beta), \ldots \Phi_{2^{\theta-1},\mathbb{M}-1}(\beta)\right]$.

Integrate (8), (9), and (10) concerning ' β ' from ' 0 ' to ' β ', we get

$$X(\beta) = X(0) + \int_0^\beta R^{\mathrm{T}}\Phi(\beta)d\beta,$$
$$Y(\beta) = Y(0) + \int_0^\beta S^{\mathrm{T}}\Phi(\beta)d\beta,$$
$$Z(\beta) = Z(0) + \int_0^\beta T^{\mathrm{T}}\Phi(\beta)d\beta,$$

Again, we can also define the initial condition with the help of the wavelets using $\Phi(\beta)$ in terms of known vectors D, E, and F as;

$$\left.\begin{array}{l} X(\beta) = D^T\Phi(\beta) + R^T[P\Phi(\beta) + \overline{\Phi}(\beta)] \\ Y(\beta) = E^T\Phi(\beta) + S^T[P\Phi(\beta) + \overline{\Phi}(\beta)] \\ Z(\beta) = F^T\Phi(\beta) + T^T[P\Phi(\beta) + \overline{\Phi}(\beta)] \end{array}\right\}. \tag{11}$$

Put (8), (9), (10), and (11) in (1) to get,

$$\left.\begin{array}{c} R^T\Phi(\beta) - \rho + \alpha\left(D^T\Phi(\beta) + R^T[P\Phi(\beta) + \overline{\Phi}(\beta)]\right) - \kappa\left(D^T\Phi(\beta) + R^T[P\Phi(\beta) + \overline{\Phi}(\beta)]\right) \\ \left(\frac{1}{X_{max}}\right)\left(X_{\max} - D^T\Phi(\beta) - R^T[P\Phi(\beta) + \overline{\Phi}(\beta)] - E^T\Phi(\beta) - S^T[P\Phi(\beta) + \overline{\Phi}(\beta)]\right) \\ +\eta\left(F^T\Phi(\beta) + C^T[P\Phi(\beta) + \overline{\Phi}(\beta)]\right)\left(D^T\Phi(\beta) + R^T[P\Phi(\beta) + \overline{\Phi}(\beta)]\right) = 0 \\ S^T\Phi(\beta) + \eta\left(F^T\Phi(\beta) + T^T[P\Phi(\beta) + \overline{\Phi}(\beta)]\right)\left(D^T\Phi(\beta) + R^T[P\Phi(\beta) + \overline{\Phi}(\beta)]\right) \\ +e\left(E^T\Phi(\beta) + S^T[P\Phi(\beta) + \overline{\Phi}(\beta)]\right) = 0. \\ T^T\Phi(\beta) - le\left(E^T\Phi(\beta) + S^T[P\Phi(\beta) + \overline{\Phi}(\beta)]\right) + \zeta\left(F^T\Phi(\beta) + T^T[P\Phi(\beta) + \overline{\Phi}(\beta)]\right) = 0\cdot \end{array}\right\} \tag{12}$$

Hence using the grid points $\beta_i = \frac{2i-1}{2\mathbb{M}}, \quad i = 1, 2, \ldots, \mathbb{M}$ collocate each equation in (12) to get a system of $3\mathbb{M}$ number of nonlinear algebraic equations as:

$$\left.\begin{array}{c} R^T\Phi(\beta_i) - \rho + \alpha\left(D^T\Phi(\beta_i) + R^T[P\Phi(\beta_i) + \overline{\Phi}(\beta_i)]\right) - \kappa\left(D^T\Phi(\beta_i) + R^T[P\Phi(\beta_i) + \overline{\Phi}(\beta_i)]\right) \\ \left(\frac{1}{X_{max}}\right)\left(X_{\max} - D^T\Phi(\beta_i) - R^T[P\Phi(\beta_i) + \overline{\Phi}(\beta_i)] - E^T\Phi(\beta_i) - S^T[P\Phi(\beta_i) + \overline{\Phi}(\beta_i)]\right) \\ +\eta\left(F^T\Phi(\beta_i) + C^T[P\Phi(\beta_i) + \overline{\Phi}(\beta_i)]\right)\left(D^T\Phi(\beta_i) + R^T[P\Phi(\beta_i) + \overline{\Phi}(\beta_i)]\right) = 0 \\ S^T\Phi(\beta_i) + \eta\left(F^T\Phi(\beta_i) + T^T[P\Phi(\beta_i) + \overline{\Phi}(\beta_i)]\right)\left(D^T\Phi(\beta_i) + R^T[P\Phi(\beta_i) + \overline{\Phi}(\beta_i)]\right) \\ +e\left(E^T\Phi(\beta_i) + S^T[P\Phi(\beta_i) + \overline{\Phi}(\beta_i)]\right) = 0. \\ T^T\Phi(\beta_i) - le\left(E^T\Phi(\beta_i) + S^T[P\Phi(\beta_i) + \overline{\Phi}(\beta_i)]\right) + \zeta\left(F^T\Phi(\beta_i) + T^T[P\Phi(\beta_i) + \overline{\Phi}(\beta_i)]\right) = 0\cdot \end{array}\right\} \tag{13}$$

This system of $3\mathbb{M}$ number of algebraic equations can be solved using the Newton-Raphson iterative method for the unknown wavelet coefficients. On substituting these values of the Taylor wavelet coefficients into (11), we obtain the Taylor wavelet solution (TWCM) of the given set of differential equations.

7. Application

Consider the mathematical model given in (1) under the physical conditions $X(0) = 0.1, \dot{X}(0) = 0$ and $Z(0) = 0.1$. We solve this problem under the parameter assumption $\rho = 0.1, \alpha = 0.02, e = 0.3, \kappa = 3, \zeta = 2.4, \eta = 0.0027, X_{\max} = 1500, l = 9$, and use the TWCM at multiple values of $\mathbb{M}$ specifically, $\mathbb{M} = 6, 10$ and resulting functions are defined in terms of β as an approximate solution.

$$\begin{aligned}
X_6(\beta) =& 0.1 + 0.391849314980778\beta + 0.652578569714826\beta^2 + 0.305352911248652\beta^3 \\
&+ 1.112908367827407\beta^4 - 0.574276380696896\beta^5 + 0.600245500852454\beta^6. \\
Y_6(\beta) =& 0.26927109803740110^{-04}\beta + 0.174859493819873^{-04}\beta^2 - 0.090018123930134 \times 10^{-04}\beta^3 \\
&0.068532503343592 \times 10^{-04}\beta^4 - 0.029607084090885 \times 10^{-04}\beta^5 + 0.006836809445419 \times 10^{-04}\beta^6. \\
Z_6(\beta) =& 0.1 - 0.239930028033178\beta + 0.287163852666480\beta^2 - 0.225793198953596\beta^3 \\
&0.125350261037950\beta^4 - 0.046066799809311\beta^5 + 0.008375595715552\beta^6.
\end{aligned}$$

Again, the Taylor wavelet approximate solution can be obtained for $\mathbb{M} = 10$ as;

$$\begin{aligned}
X_{10}(\beta) =& 0.1 + 0.397952585375662\beta + 0.592857405152523\beta^2 + 0.588631170910021\beta^3 + 0.438833723264729\beta^4 + \\
&0.258747731575785\beta^5 + 0.134718839752166\beta^6 + 0.044976485213545\beta^7 - 0.031472139619475 \times 10^{-4}\beta^8 \\
&- 0.001849090990152\beta^9 + 0.005253753938138\beta^{10}. \\
Y_{10}(\beta) =& 0.269999971410632 \times 10^{-04}\beta + 0.172736714738806 \times 10^{-04}\beta^2 - 0.084056242865232 \times 10^{-04}\beta^3 + \\
&0.061466882585223 \times 10^{-04}\beta^4 - 0.028374283467235 \times 10^{-04}\beta^5 + 0.011526511266758 \times 10^{-04}\beta^6 \\
&- 0.003888503584565 \times 10^{-04}\beta^7 + 0.001144412865512 \times 10^{-04}\beta^8 - 0.000251503853561 \times 10^{-04}\beta^9 \\
&- 0.000037603138067 \times 10^{-04}\beta^{10}. \\
Z_{10}(\beta) =& 0.1 - 0.239999991710964\beta + 0.288036263222978\beta^2 - 0.230411617444864\beta^3 + 0.138230037967910\beta^4 - \\
&0.066303550094900\beta^5 + 0.026408822903378\beta^6 - 0.008863392956058\beta^7 + 0.002442548239049\beta^8 \\
&- 0.000495202499617\beta^9 + 0.000054021311694\beta^{10}.
\end{aligned}$$

Figure 1, 2, 3 shows the comparison of the approximate solution of TWCM with the analytical solution graphically for $X(\beta), Y(\beta)$ and $Z(\beta)$, respectively while Figures 4, 5, 6 shows that the absolute error occurred in TWCM is much closure to the x-axis than several other methods for $X(\beta), Y(\beta)$ and $Z(\beta)$, respectively. Similarly, Table 1, 2, 3 are placed to compare the outcomes of the TWCM with several other methods for $X(\beta), Y(\beta)$ and $Z(\beta)$, respectively while Tables 4, 5, 6 displays the TWCM absolute error statistics and how they relate to the absolute errors of other known methods i.e Haar method, for $X(\beta), Y(\beta)$ and $Z(\beta)$, respectively.

Table 1: Taylor wavelet solution comparison with some available methods for X.

β	Taylor wavelet at $\mathbb{M} = 10$	Analytic solution	Runge-Kutta	Haar wavelet at J = 5	LADM [19]	LADM-pade [19]
0.0	0.1	0.1	0.1	0.1	0.1	0.1
0.1	0.146359074139530	0.1463590954390	0.1463590819784	0.1464175305555	0.1463590767342	0.1463590766244
0.2	0.208808073744523	0.2088080635351	0.2088080845252	0.2088998615066	0.2088073298445	0.2088072731333
0.3	0.292929399742979	0.2929294113660	0.2929294121750	0.2930706066095	0.2929159946833	0.2929137862375
0.4	0.406240523590163	0.4062403736489	0.4062405377477	0.4064543676649	0.4061358315487	0.4061052625432
0.5	0.558863332475990	0.5588631040412	0.5588633525856	0.5591827244497	0.5583427110663	0.5581020599255
0.6	0.764423864020007	0.7644235436246	0.7644238855225	0.7648968622088	0.7624762220221	0.7611467713422
0.7	1.041260776119432	1.0412603282587	1.0412608078360	1.0419569015502	1.0352712974845	1.0295183448456
0.8	1.414046790541765	1.4140461662432	1.4140468253655	1.4149122238159	1.3980828630585	1.3773198590566
0.9	1.915961149951419	1.9159602830465	1.9159611979814	1.9166641235351	1.8778035035674	1.8129744009876
1.0	2.591594743811891	2.5915957524456	2.5915948088777	2.5922241210937	2.5078741510885	2.3291697610879

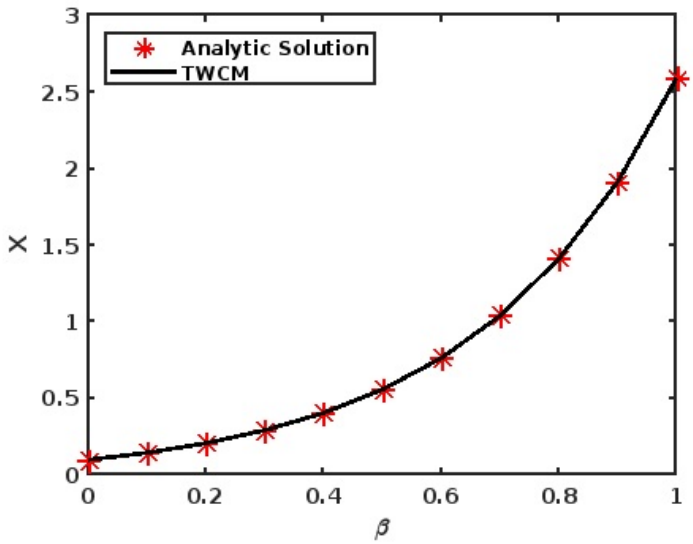

Figure 1: Approximate solution using Taylor wavelets and analytic solution comparison for X.

Table 2: Taylor wavelet solution comparison with some available methods for Y.

β	Taylor wavelet at $\mathbb{M} = 10$	Analytic solution	Runge-Kutta	Haar wavelet at J = 5	LADM [19]	LADM-pade [19]
0.0	0	0	0	0	0	0
0.1	0.0286491821e-04	0.0000028649198	0.0000028649252	0.0000028674043	0.0000028649189	0.0000028649189
0.2	0.0603269708e-04	0.0000060327036	0.0000060327021	0.0000060368541	0.0000060327069	0.0000060327072
0.3	0.0947133322e-04	0.0000094713566	0.0000094713552	0.0000094773870	0.0000094714323	0.0000094714472
0.4	0.1315827925e-04	0.0000131583444	0.0000131583407	0.0000131664732	0.0000131589100	0.0000131591617
0.5	0.1707858565e-04	0.0000170787402	0.0000170787355	0.0000170891907	0.0000170813741	0.0000170841716
0.6	0.2122346176e-04	0.0000212237911	0.0000212237850	0.0000212367950	0.0000212329817	0.0000212683688
0.7	0.2558917453e-04	0.0000255898231	0.0000255898156	0.0000256056241	0.0000256161463	0.0000254183417
0.8	0.3017622375e-04	0.0000301774286	0.0000301774195	0.0000301963391	0.0000302427015	0.0000300691867
0.9	0.3498875105e-04	0.0000349908913	0.0000349908805	0.0000350132468	0.0000351358962	0.0000348647969
1.0	0.4003415622e-04	0.0000400378278	0.0000400378146	0.0000400630524	0.0000403332185	0.0000398736542

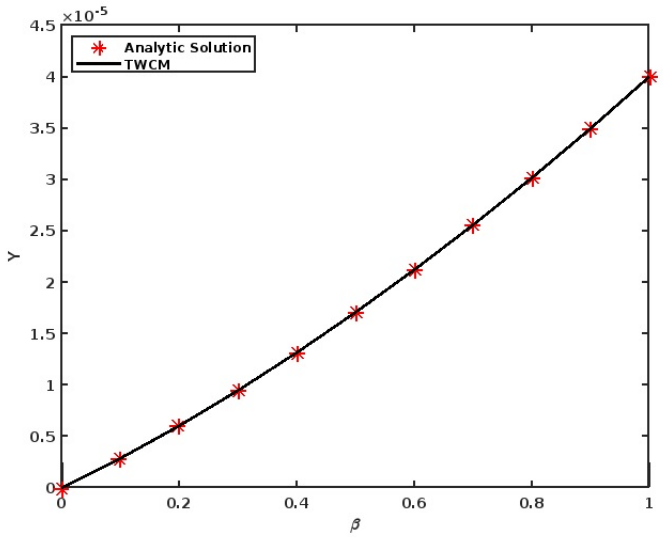

Figure 2: Approximate solution using Taylor wavelets and analytic solution comparison for Y.

Table 3: Taylor wavelet solution comparison with some available methods for Z.

β	Taylor wavelet at $\mathbb{M} = 10$	Analytic solution	Runge-Kutta	Haar wavelet at J = 5	LADM [19]	LADM-pade [19]
0.0	0.1	0.1	0.1	0.1	0.1	0.1
0.1	0.078663137358404	0.0786631825201	0.0786631763321	0.0786747964168	0.0786631771622	0.0786631770757
0.2	0.061879692890033	0.0618798440184	0.0618798433073	0.0618872437681	0.0618799530567	0.0618799602595
0.3	0.048678162621944	0.0486784909571	0.0486784889977	0.0486829421885	0.0486803130909	0.0486806266335
0.4	0.038294327888014	0.0382948815020	0.0382948878764	0.0382973184821	0.0383081804755	0.0383132488366
0.5	0.030127028569443	0.0301278673029	0.0301278739346	0.0301335302519	0.0301895642466	0.0302409705361
0.6	0.023703372572185	0.0237045441571	0.0237045501402	0.0239030930242	0.0239198160879	0.0243917434987
0.7	0.018651368339482	0.0186529155941	0.0186529209061	0.0193062210455	0.0192699954285	0.0445826889163
0.8	0.014678396597194	0.0146803591209	0.0146803637634	0.0142131736502	0.0162123434366	0.0099672189344
0.9	0.011554275444768	0.0115566903957	0.0115566944064	0.0115583240985	0.0149648655605	0.0069108403314
1.0	0.009097938938606	0.0091008452186	0.0091008450579	0.0093183517456	0.0160550223855	0.0033050764474

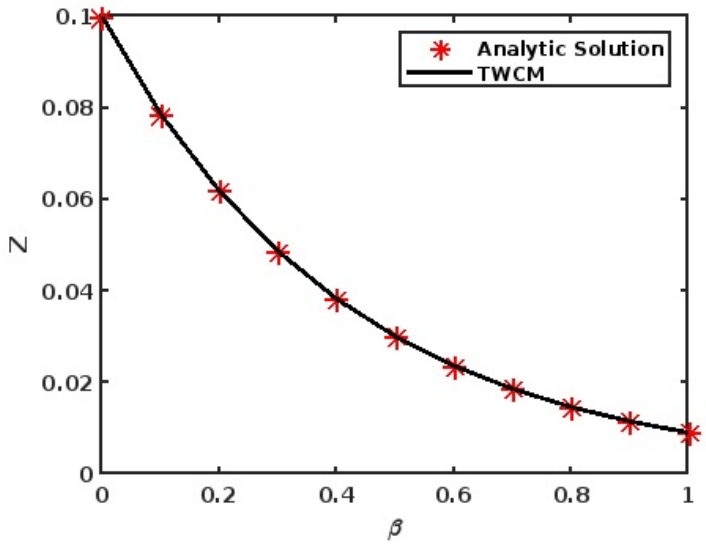

Figure 3: Approximate solution using Taylor wavelets and analytic solution comparison for Z.

Table 4: Error variance in X along with various $\mathbb{M}$ values.

β	Analytic Solution	Taylor wavelet at $\mathbb{M} = 6$	Taylor wavelet at $\mathbb{M} = 9$	Haar wavelet at J = 5	AE at $\mathbb{M} = 6$	AE at $\mathbb{M} = 9$	AE in Haar solution
0.0	0.1	0.1	0.1	0.1	0	0	0
0.2	0.2088080635351	0.208551129733493	0.208808073744523	0.2088998615066	2.5693e-04	1.0209e-08	9.179714e-05
0.4	0.4062403736489	0.405763353116134	0.406240523590163	0.4064543676649	4.7702e-04	1.4994e-07	2.139940e-05
0.6	0.7644235436246	0.763576350110727	0.764423864020007	0.7648968622088	8.4719e-04	3.2040e-07	4.733185e-04
0.8	1.4140461662432	1.412489566772234	1.414046790541765	1.4149122238159	1.5566e-03	6.2430e-07	8.660575e-04
1.0	2.5915957524456	2.588658283927222	2.591594743811891	2.5922241210937	2.9375e-03	1.0086e-06	6.283686e-04

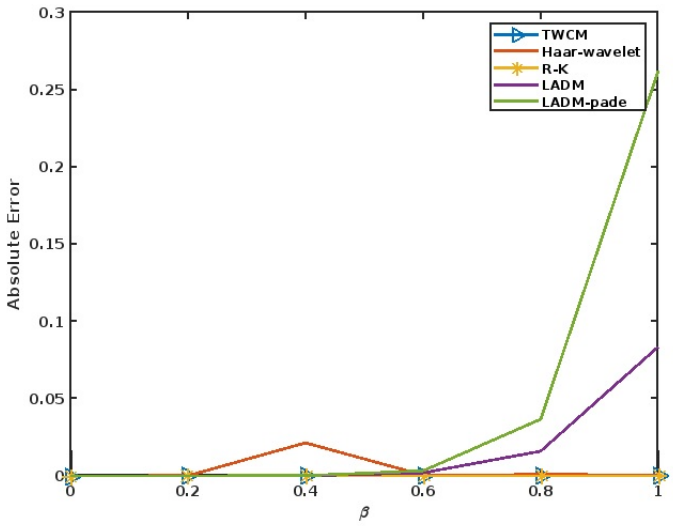

Figure 4: Absolute error comparison of TWCM with Haar wavelet, Runge-Kutta method, LADM method [19] and LADM-pade method [19] for X.

Table 5: Error variance in Y along with various $\mathbb{M}$ values.

β	Analytic solution	Taylor wavelet at $\mathbb{M} = 6$	Taylor wavelet at $\mathbb{M} = 9$	Haar wavelet at J = 5	AE at $\mathbb{M} = 6$	AE at $\mathbb{M} = 9$	AE in Haar solution
0.0	0	0	0	0	0	0	0
0.2	0.0000060327036	0.06022906968e-04	0.0603269708e-04	0.0000060368541	9.7966e-09	6.5101e-12	4.150499e-09
0.4	0.0000131583444	0.13140405748e-04	0.1315827925e-04	0.0000131664732	1.7939e-08	6.5141e-11	8.128791e-09
0.6	0.0000212237911	0.21196670558e-04	0.2122346176e-04	0.0000212367950	2.7121e-08	3.2934e-10	1.300390e-08
0.8	0.0000301774286	0.30139916768e-04	0.3017622375e-04	0.0000301963391	3.7512e-08	1.2048e-09	1.891049e-08
1.0	0.0000400378278	0.39987469668e-04	0.4003415622e-04	0.0000400630524	5.0358e-08	3.6716e-09	2.522460e-08

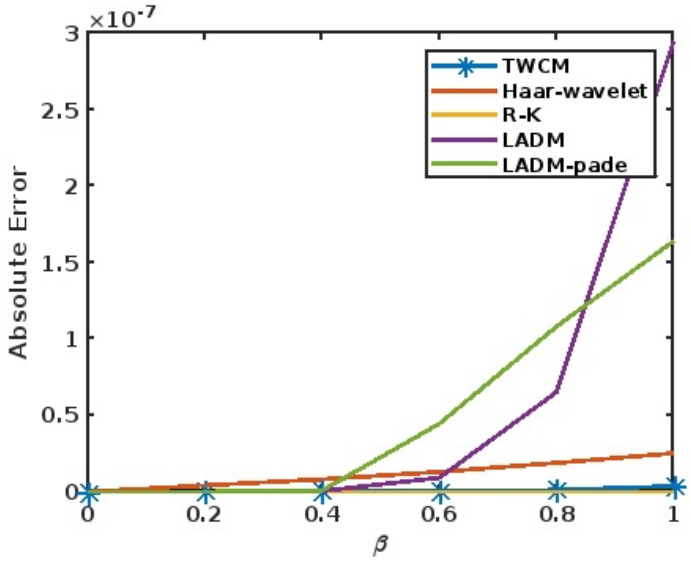

Figure 5: Absolute error comparison of TWCM with Haar wavelet, Runge-Kutta method, LADM method [19] and LADM-pade method [19] for Y.

Table 6: Error variance in Z along with various $\mathbb{M}$ values.

β	Analytic solution	Taylor wavelet at $\mathbb{M} = 6$	Taylor wavelet at $\mathbb{M} = 9$	Haar wavelet at J = 5	AE at $\mathbb{M} = 6$	AE at $\mathbb{M} = 9$	AE in Haar Method
0.0	0.1	0.1	0.1	0.1	0	0	0
0.2	0.0618798440184	0.061880557988242	0.061879692890033	0.0618872437681	7.1397e-07	1.5113e-07	7.399749e-06
0.4	0.0382948815020	0.038294989572911	0.038294327888014	0.0382973184821	1.0807e-07	5.5361e-07	2.436980e-06
0.6	0.0237045441571	0.023703650437101	0.023703372572185	0.0239030930242	8.9372e-07	1.1716e-06	1.985488e-04
0.8	0.0146803591209	0.014678635538651	0.014678396597194	0.0142131736502	1.7236e-06	1.9625e-06	4.671854e-04
1.0	0.0091008452186	0.009099682623898	0.009097938938606	0.0093183517456	1.1626e-06	2.9063e-06	2.175065e-04

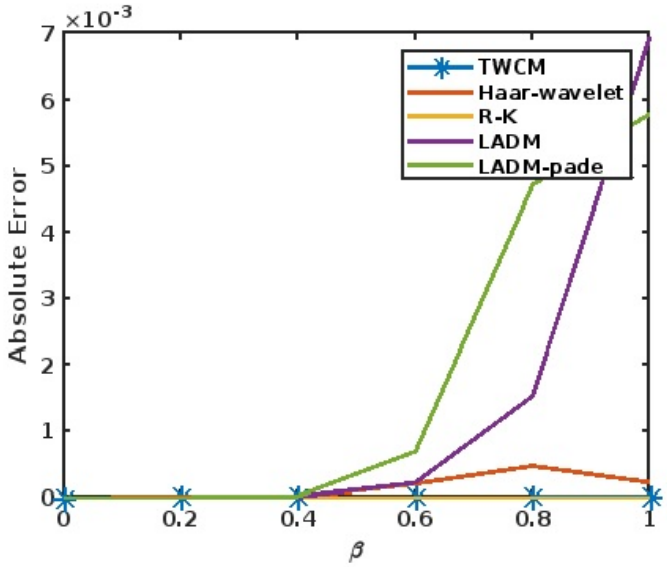

Figure 6: Absolute error comparison of TWCM with Haar wavelet, Runge-Kutta method, LADM method [19] and LADM-pade method [19] for Z.

8. Conclusion

In this study, we have presented and studied a new mathematical model representing the spreading behavior of a very serious disease HIV infection. The model is numerically solved using a new wavelet method-based analysis including some operations of MATLAB software. The outcomes of the method are compared with several other existing methods under some specific values of the underlying parameters and it is shown that the method works well to handle the given problem and outcomes are more accurate than several other existing strategies of the literature. The suggested approach, which we refer to as TWCM, is used for two distinct stages, the results are compared in tabulated form, and figures are provided to prove less absolute error occurred in comparison with the precise answer than previous methods. Therefore increasing the number of truncated terms will produce a more accurate solution and reduced absolute error as well. Finally, we present some of the findings from our analysis:

1. The current method delivers greater precision than the exact solution.
2. This approach is straightforward for implementation within computer programming, and by simply performing a little alteration to the present system, we can expand it to additional problems.
3. The proposed technique also happens to be relatively simple to put into practice, and the computational findings demonstrate that it is fairly successful for computationally solving the above-mentioned mathematical frameworks along with other systems of ordinary differential equations.
4. Taylor wavelet characteristics and their convergent analysis are clarified using theoretical explanations.
5. Large operational matrix may require more operations and computation time.

9. CRediT authorship contribution statement

The fundamental concept for the article was developed by Vivek, and all authors contributed equally.

10. Declaration of competing interest

Each author hereby certifies that they don't have any conflicts of interest.

11. Data availability

NA.

12. Acknowledgments

All authors are grateful to the esteemed reviewers who participated in the review process for suggesting a great and innovative approach to not only enhance the standards of the script but also a future way to move in the right direction.

References

[1] Perelson AS. Modeling the interaction of the immune system with HIV. In Mathematical and statistical approaches to AIDS epidemiology 1989 Dec 20 (pp. 350-370). Berlin, Heidelberg: Springer Berlin Heidelberg.
[2] Kumar S, Kumar R, Singh J, Nisar KS, Kumar D. An efficient numerical scheme for fractional model of HIV-1 infection of CD4+ T-cells with the effect of antiviral drug therapy. Alexandria Engineering Journal. 2020;59(4):2053-64.
[3] Yüzbaşı Ş. A numerical approach to solve the model for HIV infection of CD4+ T cells. Applied Mathematical Modelling. 2012;36(12):5876-90.
[4] Ghoreishi M, Ismail AM, Alomari AK. Application of the homotopy analysis method for solving a model for HIV infection of CD4+ T-cells. Mathematical and Computer Modelling. 2011;54(11-12):3007-15.
[5] Merdan M. Homotopy perturbation method for solving a model for HIV infection of CD4+ T cells. İstanbul Ticaret Üniversitesi Fen Bilimleri Dergisi. 2007;6(12):39-52.
[6] Balamuralitharan S, Geetha V. Analytical approach to solve the model for hiv Infection of CD4+ T cells using LADM. International Journal of Pure and Applied Mathematics. 2017;113(11):243-51.
[7] Sweilam NH, Al-Mekhlafi SM. Legendre spectral-collocation method for solving fractional optimal control of HIV infection of CD4+ T cells mathematical model. The Journal of Defense Modeling and Simulation. 2017;14(3):273-84.
[8] Gökdoğan A, Yildirim A, Merdan M. Solving a fractional order model of HIV infection of CD4+ T cells. Mathematical and Computer Modelling. 2011;54(9-10):2132-8.
[9] Merdan M, Gökdoğan A, Yildirim A. On the numerical solution of the model for HIV infection of CD4+ T cells. Computers Mathematics with Applications. 2011;62(1):118-23.
[10] Mirzaee F, Samadyar N. On the numerical method for solving a system of nonlinear fractional ordinary differential equations arising in HIV infection of CD4+ T cells. Iranian Journal of Science and Technology, Transactions A: Science. 2019;43(3):1127-38.
[11] Mirzaee F, Samadyar N. Parameters estimation of HIV infection model of CD4+ T-cells by applying orthonormal Bernstein collocation method. International Journal of Biomathematics. 2018;11(02):1850020.
[12] Mirzaee F, Samadyar N. Convergence of 2D-orthonormal Bernstein collocation method for solving 2D-mixed Volterra–Fredholm integral equations. Transactions of A. Razmadze Mathematical Institute. 2018;172(3):631-41.
[13] Keshavarz E, Ordokhani Y, Razzaghi M. The Bernoulli wavelets operational matrix of integration and its applications for the solution of linear and nonlinear problems in calculus of variations. Applied Mathematics and Computation. 2019;351:83-98.
[14] Kumbinarasaiah S, Mundewadi RA. The new operational matrix of integration for the numerical solution of integro-differential equations via Hermite wavelet. SeMA Journal. 2021;78(3):367-84.
[15] Hsiao CH. Haar wavelet approach to linear stiff systems. Mathematics and Computers in simulation. 2004;64(5):561-7.
[16] Ali S, Khan A, Shah K, Alqudah MA, Abdeljawad T. On computational analysis of highly nonlinear model addressing real world applications. Results in Physics. 2022;36:105431.
[17] Alrabaiah H, Ahmad I, Amin R, Shah K. A numerical method for fractional variable order pantograph differential equations based on Haar wavelet. Engineering with Computers. 2022:1-4.
[18] Kumbinarasaiah S. Hermite wavelets approach for the multi-term fractional differential equations. Journal of Interdisciplinary Mathematics. 2021;24(5):1241-62.
[19] Ongun MY. The Laplace Adomian decomposition method for solving a model for HIV infection of CD4+ T cells. Mathematical and Computer Modelling. 2011;53(5-6):597-603.
[20] Lepik Ü. Application of the Haar wavelet transform to solving integral and differential equations. InProceedings of the Estonian Academy of Sciences, Physics, Mathematics 2007 (Vol. 56, No. 1).
[21] Srivastava HM, Irfan M, Shah FA. A Fibonacci wavelet method for solving dual-phase-lag heat transfer model in multi-layer skin tissue during hyperthermia treatment. Energies. 2021;14(8):2254.
[22] Shah FA, Irfan M, Nisar KS, Matoog RT, Mahmoud EE. Fibonacci wavelet method for solving time-fractional telegraph equations with Dirichlet boundary conditions. Results in Physics. 2021;24:104123.
[23] Jan A, Srivastava HM, Khan A, Mohammed PO, Jan R, Hamed YS. In Vivo HIV Dynamics, Modeling the Interaction of HIV and Immune System via Non-Integer Derivatives. Fractal and Fractional. 2023;7(5):361.
[24] Srivastava HM, Shah FA, Nayied NA. Fibonacci wavelet method for the solution of the non-linear Hunter–Saxton equation. Applied Sciences. 2022;12(15):7738.
[25] Izadi M, Srivastava HM. Fractional clique collocation technique for numerical simulations of fractional-order Brusselator chemical model. Axioms. 2022;11(11):654.

[26] Hadhoud AR, Srivastava HM, Rageh AA. Non-polynomial B-spline and shifted Jacobi spectral collocation techniques to solve time-fractional nonlinear coupled Burgers' equations numerically. Advances in Difference Equations. 2021;2021:1-28.
[27] Srivastava HM, Irfan M, Shah FA. A Fibonacci wavelet method for solving dual-phase-lag heat transfer model in multi-layer skin tissue during hyperthermia treatment. Energies. 2021;14(8):2254.
[28] Srivastava HM, Alomari AK, Saad KM, Hamanah WM. Some dynamical models involving fractional-order derivatives with the Mittag-Leffler type kernels and their applications based upon the Legendre spectral collocation method. Fractal and Fractional. 2021;5(3):131.
[29] Kumar S, Pandey RK, Srivastava HM, Singh GN. A convergent collocation approach for generalized fractional integro-differential equations using Jacobi poly-fractonomials. Mathematics. 2021;9(9):979.
[30] Srivastava HM, Shah FA, Abass R. An application of the Gegenbauer wavelet method for the numerical solution of the fractional Bagley-Torvik equation. Russian Journal of Mathematical Physics. 2019;26(1):77-93.
[31] Pinto CM, Carvalho AR, Baleanu D, Srivastava HM. Efficacy of the post-exposure prophylaxis and of the HIV latent reservoir in HIV infection. Mathematics. 2019;7(6):515.
[32] Vivek, Kumar M, Mishra SN. A fast Fibonacci wavelet-based numerical algorithm for the solution of HIV-infected CD4+ T cells model. The European Physical Journal Plus. 2023;138(5):458.
[33] Vivek, Kumar M, Mishra SN. Solution of linear and nonlinear singular value problems using operational matrix of integration of Taylor wavelets. Journal of Taibah University for Science. 2023;17(1):2241716.
[34] Keshavarz E, Ordokhani Y, Razzaghi M. The Taylor wavelets method for solving the initial and boundary value problems of Bratu-type equations. Applied Numerical Mathematics. 2018;128:205-16.
[35] Keshavarz E, Ordokhani Y, Razzaghi M. The Taylor wavelets method for solving the initial and boundary value problems of Bratu-type equations. Applied Numerical Mathematics. 2018;128:205-16.
[36] Kumbinarasaiah S, Adel W. Hermite wavelet method for solving nonlinear Rosenau–Hyman equation. Partial Differential Equations in Applied Mathematics. 2021;4:100062.
[37] Raghunatha KR, Kumbinarasaiah S. Laguerre wavelet numerical solution of micropolar fluid flow in a porous channel with high mass transfer. Journal of Interdisciplinary Mathematics. 2021;24(8):2269-82.